In Vivo Role of Focal Adhesion Kinase in Regulating Pancreatic β-Cell Mass and Function Through Insulin Signaling, Actin Dynamics, and Granule Trafficking

Erica P. Cai,[1,2] Marina Casimir,[3] Stephanie A. Schroer,[2] Cynthia T. Luk,[1,2] Sally Yu Shi,[1,2] Diana Choi,[1] Xiao Qing Dai,[3] Catherine Hajmrle,[3] Aliya F. Spigelman,[3] Dan Zhu,[4,5] Herbert Y. Gaisano,[1,4,5] Patrick E. MacDonald,[3] and Minna Woo[1,2,4,6]

Focal adhesion kinase (FAK) acts as an adaptor at the focal contacts serving as a junction between the extracellular matrix and actin cytoskeleton. Actin dynamics is known as a determinant step in insulin secretion. Additionally, FAK has been shown to regulate insulin signaling. To investigate the essential physiological role of FAK in pancreatic β-cells in vivo, we generated a transgenic mouse model using rat insulin promoter (RIP)–driven Cre-loxP recombination system to specifically delete FAK in pancreatic β-cells. These RIPcre^{+}*fak*$^{fl/fl}$ mice exhibited glucose intolerance without changes in insulin sensitivity. Reduced β-cell viability and proliferation resulting in decreased β-cell mass was observed in these mice, which was associated with attenuated insulin/Akt (also known as protein kinase B) and extracellular signal–related kinase 1/2 signaling and increased caspase 3 activation. FAK-deficient β-cells exhibited impaired insulin secretion with normal glucose sensing and preserved Ca^{2+} influx in response to glucose, but a reduced number of docked insulin granules and insulin exocytosis were found, which was associated with a decrease in focal proteins, paxillin and talin, and an impairment in actin depolymerization. This study is the first to show in vivo that FAK is critical for pancreatic β-cell viability and function through regulation in insulin signaling, actin dynamics, and granule trafficking. ***Diabetes*** **61:1708–1718, 2012**

Focal adhesion kinase (FAK) was discovered in 1992 as a nonreceptor tyrosine kinase that is involved in integrin signaling (1). Integrins engage with the extracellular matrix (ECM) and recruit FAK to form dynamic structures known as focal adhesions. Signaling between cell adhesion receptors, integrins, and the ECM can deliver signals from either intra- or extracellular environments to influence tissue development, cell viability, and motility. Additionally, FAK, along with paxillin and talin, has been shown to regulate intracellular cytoskeleton dynamics (2). Actin reorganization is important during insulin release (3,4). Upon glucose stimulation, the cortical filamentous actin (F-actin)–organized web is disassembled through depolymerization, permitting insulin granules to approach the plasma membrane and interact with target membrane–soluble *N*-ethylmaleimide attachment protein receptor (t-SNARE) proteins to achieve exocytosis (3).

The structure of FAK consists of three domains: an NH_2-terminal protein 4.1, ezrin, radixin, and moesin homology (FERM) domain, a central kinase domain, and a COOH-terminal focal adhesion–targeting domain (5). The FERM domain associates with integrin molecules while the tyrosine residue 397 of the focal adhesion–targeting domain autophosphorylates upon stimulation by integrins. Activated FAK can subsequently phosphorylate other FAK tyrosine residues and associated Src homology 2 domain–containing proteins, such as Src and the p85 subunit of phosphatidylinositol 3-kinase (PI3K) (6).

In vivo small interfering RNA (siRNA) knockdown of FAK causes insulin resistance in liver and muscle by attenuating phosphorylation of insulin receptor substrate 1 (IRS1) (7). Similarly, antisense FAK in a cultured muscle cell line prevented actin reorganization, resulting in decreased GLUT4 translocation and downregulation of insulin/Akt (also known as protein kinase B) signaling (8), whereas increased FAK expression in an insulin-resistant muscle cell line enhanced insulin sensitivity and glucose uptake (9). Recently, phosphorylation of FAK and paxillin was shown to be crucial for glucose-stimulated insulin secretion in primary β-cells in vitro (10). However, the in vivo role of FAK in pancreatic β-cells and whole-body glucose homeostasis remains unknown.

In the current study, we used a transgenic mouse model to determine the in vivo role of FAK in pancreatic β-cells. A Cre-loxP recombination system was used with a rat insulin promoter (RIP)–driven Cre transgene, which specifically deletes FAK in pancreatic β-cells. Our results show that β-cell–specific FAK knockout (RIPcre^{+}*fak*$^{fl/fl}$) mice exhibit reduced β-cell mass due to increased apoptosis and decreased proliferation under basal conditions. Additionally, mice had β-cell dysfunction, as evidenced by reduced insulin secretion due to suppressed focal adhesion protein, paxillin activation, and talin expression and impaired F-actin depolymerization and insulin granule trafficking. Altogether, this study is the first to show an essential in vivo role of FAK in the maintenance of pancreatic β-cell mass and function. The absence of FAK in β-cells leads to abnormal glucose homeostasis due to multiple defects, including impaired cell survival, proliferation, and function through dysregulated insulin signaling and actin dynamics.

RESEARCH DESIGN AND METHODS

Mouse protocol. RIPcre^{+} mice (11) were bred to *fak*$^{fl/fl}$ mice (a gift of Dr. Louis Reichardt, University of California, San Francisco, CA) to generate RIPcre^{+}*fak*$^{+/fl}$, which were then intercrossed to generate β-cell–specific FAK

From the [1]Institute of Medical Science, University of Toronto, Toronto, Ontario, Canada; the [2]Toronto General Research Institute, Toronto, Ontario, Canada; the [3]Alberta Diabetes Institute, University of Alberta, Edmonton, Alberta, Canada; the [4]Department of Medicine, University of Toronto, Toronto, Ontario, Canada; the [5]Department of Physiology, University of Toronto, Toronto, Ontario, Canada; and the [6]Department of Medicine, St. Michael's Hospital, Toronto, Ontario, Canada.

Corresponding author: Minna Woo, mwoo@uhnres.utoronto.ca, or Patrick E. MacDonald, pmacdonald@ualberta.ca.

Received 25 September 2011 and accepted 24 February 2012.

DOI: 10.2337/db11-1344

E.P.C. and M.C. contributed equally to this study.

knockout mice (RIPcre$^+$*fak*$^{fl/fl}$). RIPcre$^+$*fak*$^{+/+}$ littermates were used as controls, and both male and female mice were used in similar number for all experiments, with the exception of streptozotocin (STZ) experiments, where only male mice were used to avoid potential confounding effects of estrogen in β-cells (12). Genotypes for *cre* and *fak* genes were determined by PCR using ear clip DNA. All mice were maintained on a C57BL/6 background and housed in a pathogen-free animal facility with a 12-h light-dark cycle and fed standard irradiated rodent chow (5% fat; Harlan Tekad, Indianapolis, IN). All animal experimental protocols were approved by the Ontario Cancer Institute Animal Care Facility.

Metabolic studies. Glucose tolerance tests (GTTs) were performed on overnight-fasted (14–16 h) mice by intraperitoneal injection of glucose (1 g/kg of body weight), and blood glucose levels were measured at 0, 15, 30, 45, 60, and 120 min after glucose injection by glucose meter (Precision Xtra; Abbott Laboratories). Insulin tolerance tests were performed on overnight-fasted mice using human recombinant insulin (Novolin R; Novo Nordisk) at a dose of 1 unit/kg of body weight, and blood glucose levels were measured at 0, 15, 30, 45, and 60 min. The mice that were used were 4–8 and 12–18 weeks old.

Immunohistochemistry and immunofluorescent staining. The pancreas was isolated from 4–8- and 12–18-week-old mice as described in previous studies (13–15). Paraffin-embedded sections at three levels 150 μm apart were immunostained for insulin, Ki67 (DAKO), glucagon (Cell Signaling), and GLUT2 (Millipore). Immunofluorescent images were obtained by a Zeiss inverted fluorescent microscope (Advanced Optical Microscopy Facility, Toronto, Ontario, Canada). Immunohistochemically stained pancreatic sections for insulin or glucagon were scanned by ScanScope ImageScope system at ×20 magnifications and analyzed with ImageScope version 9.0.19.1516 software (Aperio Technologies, Vista, CA) for β- and α-cell area. Cell mass was calculated by β- or α-cell area multiplied by whole pancreas weight. Ki67-positive cells were manually counted on immunohistochemically stained pancreatic sections as percentages of total islet cells (~250 islets were counted from each animal). Pancreatic sections were stained with hematoxylin and eosin (H&E) and imaged by light microscopy (Leica Microsystems, Inc.).

In vivo STZ-induced β-cell toxicity and transferase-mediated dUTP nick-end labeling assay. Male mice (6–8 weeks) were injected intraperitoneally with STZ (40 mg/kg of body weight) for three consecutive days and then killed for pancreas isolation. β-Cell apoptosis was assessed by transferase-mediated dUTP nick-end labeling (TUNEL) assay (Roche Biochemicals) according to the manufacturer's protocol and imaged by a Zeiss inverted fluorescent microscope (Advanced Optical Microscopy Facility).

Western blotting. Protein lysates of isolated islets, liver, muscle, and hypothalami were isolated from 4–8-week-old mice, separated by SDS-PAGE, and immunoblotted with antibodies for FAK, IR, IRS2, pIRS1/2, p27, phospho-paxillin (Tyr 118), B-cell lymphoma-extra large (Bcl-xL), cyclin-dependent kinase 5 (CDK5), talin (Santa Cruz Biotechnology), phospho-IR (Tyr 1158/1162/1163) (BioSource), paxillin (BioLegend), Bcl-2 (Calbiochem), phospho-Akt (Ser 473), Akt, p53, phospho-extracellular signal–related kinase 1/2 (phospho-ERK1/2) (Thr202/Tyr 204), ERK1/2, pancreatic and duodenal homeobox 1 (PDX-1), cleaved caspase 3, cyclin D1, and glyceraldehyde-3-phosphate dehydrogenase (Cell Signaling) as previously described (14–16). The signal densities of Western blots were quantified by Quantity One software (BioRad).

Insulin secretion and insulin content. Glucose-stimulated insulin secretion was measured on overnight-fasted 4–8-week-old mice after intraperitoneal injection of glucose (3 g/kg of body weight), from saphenous vein blood samples at 0, 2, 10, and 30 min after glucose injection. Pancreatic islets were isolated from 4–8-week-old mice, and 10 similar-sized islets per mouse were handpicked under a dissecting microscope (Leica Microsystems, Inc.). Islets were incubated overnight in RPMI 1640 media without glucose (Gibco), and 2.5 mmol/L or 15 mmol/L glucose-containing media stimulation for 30 min and then acid/ethanol extraction was performed for insulin content as previously described (15,16). Serum and media samples were assayed for insulin by ELISA (Crystal Chem, Downers Grove, IL).

Fluorescence imaging. To detect F-actin, cells were fixed with Z-FIX (Anatech Ltd., Battle Creek, MI) and stained with Alexa Fluor 488–conjugated phalloidin (Invitrogen). β-Cells were identified by insulin immunostaining (Santa Cruz Biotechnology). Cell images were captured with a Zeiss AxioCamHRm and acquired with AxioVision 4.8 imaging software (Carl Zeiss MicroImaging). Data were analyzed using ImageJ software (version 1.41o; NIH) by averaging the two peak-intensity line scans after image background subtraction.

For intracellular Ca^{2+} measurements, islets were incubated for 45 min with 3 μmol/L Fura-2-AM (Fura-2-acetoxymethyl ester) (Invitrogen) and 0.06% pluronic acid (Invitrogen) in an extracellular calcium imaging solution as previously described (17). Islets were then imaged in fresh imaging solution with 0.5 mmol/L glucose and without Fura-2-AM or pluronic acid at 37°C with constant bath perfusion. Glucose (11 mmol/L) and KCl (20 mmol/L) were increased as indicated, and NaCl concentration was reduced as required. Fluorescence recordings were obtained every 5 s. Images were analyzed with Image Pro Plus version 6.2 (Media Cybernetics) or Ratio Cam software (Metamorph).

For localization of phosphorylated paxillin detection, cells were washed with PBS and fixed in 2% paraformaldehyde. Cells were coimmunostained using antiphospho-paxillin and either anti–synaptosomal-associated protein 25 (anti-SNAP25) or anti–syntaxin 1 (Sigma-Aldrich). Images were captured and colocalization coefficient analyses were performed using a laser scanning confocal imaging system (LSM510) equipped with LSM software (Carl Zeiss, Oberkochen, Germany).

Electrophysiology. Standard, whole-cell technique with sine+DC lockin function of an EPC10 amplifier and Patchmaster software (HEKA Electronics, Lambrecht/Pfalz, Germany) were used with experiments performed at 32–35°C as previously described (17). β-Cells were identified by size and the presence of a voltage-gated Na^+ current that inactivated at approximately –90 mV (except when tetrodotoxin is present).

Electron microscopy. Pancreatic islets were isolated from 4–8-week-old mice by collagenase digestion and cultured in RPMI 1640 medium without glucose for 1 h. Islets were then stimulated with 15 mmol/L glucose-containing medium or saline for 2 min and fixed in Karnovsky-style fixative at 4°C for overnight fixation as previously described (18). Sections were imaged by a Hitachi H7000 transmission electron microscope at an accelerating voltage of 75 kV.

Statistical analysis. Data are presented as means ± SEM and were analyzed by two-tailed, independent-sample Student *t* test or one-way ANOVA, as appropriate. *P* values <0.05 were considered as statistically significant.

RESULTS

Specific deletion of FAK in β-cells and glucose homeostasis. FAK was efficiently deleted in pancreatic islets of RIPcre$^+$*fak*$^{fl/fl}$ mice as confirmed by Western blot (Fig. 1*A*). A minimal residual expression of FAK protein in islets likely represents expression in non–β-cells. Insulin promoter activity has also been shown to be present in the hypothalamus (19); therefore, FAK expression levels were also examined in isolated hypothalami, in addition to other metabolic tissues including the liver and skeletal muscle. We confirmed that FAK expression was not diminished in these tissues in RIPcre$^+$*fak*$^{fl/fl}$ mice compared with RIPcre$^+$*fak*$^{+/+}$ littermates (Fig. 1*A*). RIPcre$^+$*fak*$^{fl/fl}$ mice were healthy and born at the expected Mendelian ratio. Body weight was similar between RIPcre$^+$*fak*$^{fl/fl}$ and RIPcre$^+$*fak*$^{+/+}$ littermates (Fig. 1*B*).

We next assessed the effects of FAK deletion in the pancreatic β-cells on glucose homeostasis. Random blood glucose levels, measured in 4–8- and 12–18-week-old mice, showed an increase in RIPcre$^+$*fak*$^{fl/fl}$ compared with their RIPcre$^+$*fak*$^{+/+}$ littermates in both age-groups (Fig. 1*C*). We then performed GTTs, which demonstrated similar fasting blood glucose levels but impaired glucose tolerance in RIPcre$^+$*fak*$^{fl/fl}$ mice compared with RIPcre$^+$*fak*$^{+/+}$ controls in both age-groups (Fig. 1*D*). To investigate whether the impaired glucose tolerance was due to changes in peripheral insulin sensitivity, ITTs were performed. The results showed similar blood glucose lowering after insulin injection between RIPcre$^+$*fak*$^{+/+}$ and RIPcre$^+$*fak*$^{fl/fl}$ mice in both age-groups (Fig. 1*E*), which suggests that the impaired glucose tolerance in RIPcre$^+$*fak*$^{fl/fl}$ mice was not due to changes in peripheral insulin sensitivity but rather due to defects in β-cell mass and/or function. These results show that FAK in β-cells plays an essential role in regulating glucose homeostasis.

Reduced β-cell mass in RIPcre$^+$fak$^{fl/fl}$ mice due to decreased proliferation and increased apoptosis. β-Cell area was measured by morphometric assessment on insulin-immunostained pancreatic sections. RIPcre$^+$*fak*$^{fl/fl}$ mice showed reduced β-cell area relative to pancreatic area and β-cell mass compared with RIPcre$^+$*fak*$^{+/+}$ controls in both age-groups (Fig. 2*A* and *B*). Diminished β-cell mass in RIPcre$^+$*fak*$^{fl/fl}$ mice could arise from changes in β-cell

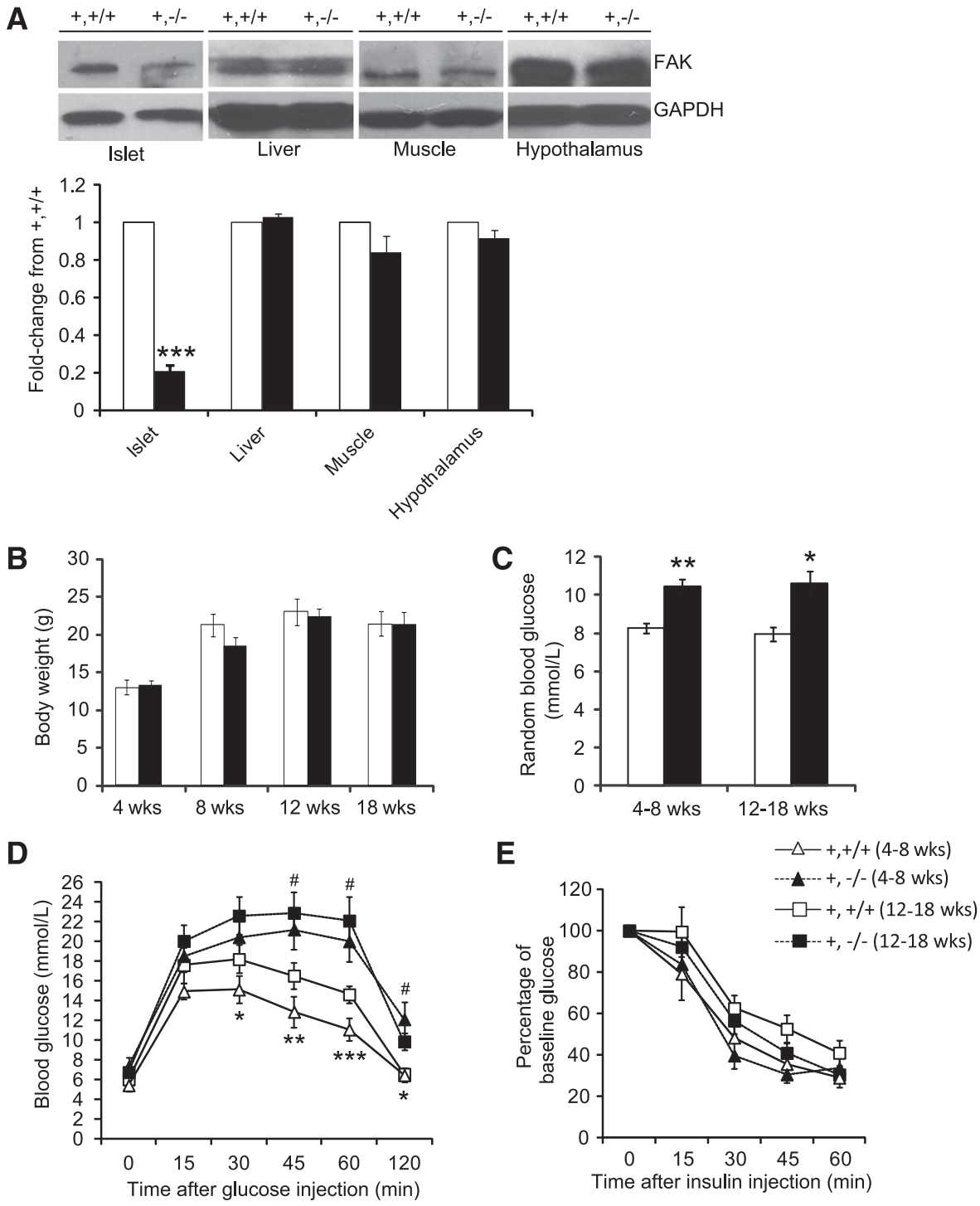

FIG. 1. Specific deletion of FAK in the pancreatic β-cells causes glucose intolerance without changes in insulin sensitivity. *A*: FAK expression in protein lysates of isolated islets of RIPcre$^+$*fak*$^{fl/fl}$ mice. The expression was not affected in liver, muscle, and hypothalamus between RIPcre$^+$*fak*$^{fl/fl}$ (■) and RIPcre$^+$*fak*$^{+/+}$ mice (□), as shown by Western blot; *n* = 3 per genotype. GAPDH, glyceraldehyde-3-phosphate dehydrogenase. *B*: Similar body weight between RIPcre$^+$*fak*$^{+/+}$ (□) and RIPcre$^+$*fak*$^{fl/fl}$ mice (■); *n* >10 per genotype. *C*: Increased random blood glucose levels in RIPcre$^+$*fak*$^{fl/fl}$ mice (■) compared with RIPcre$^+$*fak*$^{+/+}$ (□); *n* = 5 per genotype. *D*: RIPcre$^+$*fak*$^{fl/fl}$ mice display glucose intolerance compared with RIPcre$^+$*fak*$^{+/+}$ littermates in both age-groups, as assessed by GTT; *n* = 7–10 per genotype. *E*: Similar peripheral insulin sensitivity as assessed by insulin tolerance test between RIPcre$^+$*fak*$^{+/+}$ and RIPcre$^+$*fak*$^{fl/fl}$ mice; *n* = 10 per genotype. △, 4–8-week-old RIPcre$^+$*fak*$^{+/+}$; ▲, 4–8-week-old RIPcre$^+$*fak*$^{fl/fl}$; □, 12–18-week-old RIPcre$^+$*fak*$^{+/+}$; ■, 12–18-week-old RIPcre$^+$*fak*$^{fl/fl}$. *Comparison between 4–8-week-old RIPcre$^+$*fak*$^{+/+}$ and RIPcre$^+$*fak*$^{fl/fl}$ islets. #Comparison between 12–18-week-old RIPcre$^+$*fak*$^{+/+}$ and RIPcre$^+$*fak*$^{fl/fl}$ islets. *,#$P < 0.05$; **$P < 0.01$; ***$P < 0.001$. Results represent mean ± SE. +,+/+RIPcre$^+$ *fak*$^{+/+}$; +,−/−RIPcre$^+$ *fak*$^{fl/fl}$.

proliferation or viability. Immunostaining for Ki67, a marker of proliferation, on pancreatic sections showed a decreased number of Ki67-positive cells in islets of RIPcre$^+$*fak*$^{fl/fl}$ mice compared with littermate RIPcre$^+$*fak*$^{+/+}$ controls (Fig. 2*C*). We next examined for apoptosis and observed an increase in cleaved (activated) caspase 3 expression in isolated islets and TUNEL-positive, insulin-immunostained cells in pancreatic sections of RIPcre$^+$*fak*$^{fl/fl}$ mice compared with

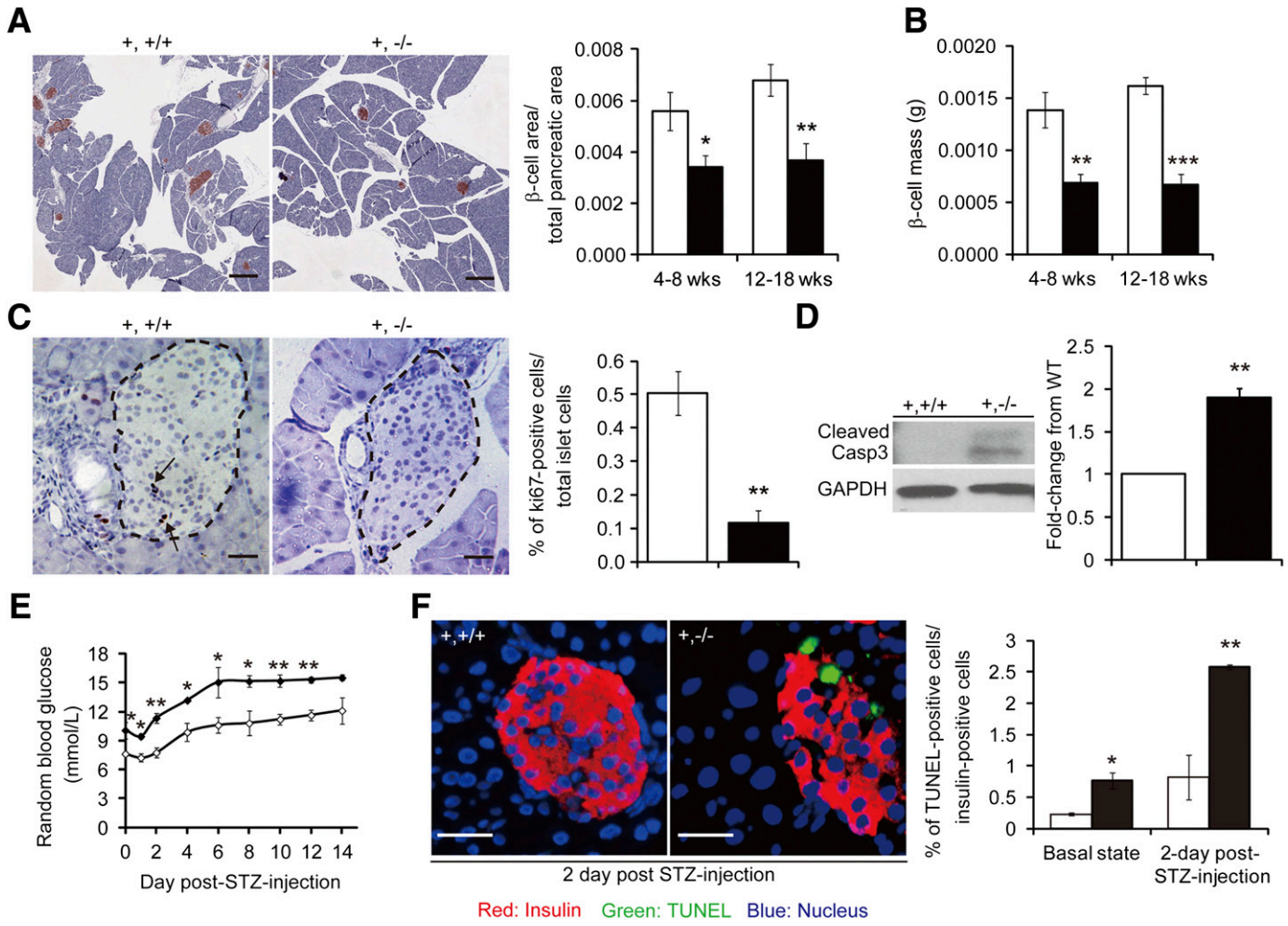

FIG. 2. Reduced cell mass in FAK-deficient β-cells due to decreased proliferation and enhanced susceptibility to apoptosis. *A*: Insulin-immunostained pancreatic sections revealed a significant reduction in β-cell area per pancreatic area in RIPcre^{+}*fak*$^{fl/fl}$ mice (■) compared with RIPcre^{+}*fak*$^{+/+}$ littermates (□); *n* = 5 per genotype. Scale bars, 200 μm. *B*: β-Cell mass was reduced in RIPcre^{+}*fak*$^{fl/fl}$ mice (■) compared with RIPcre^{+}*fak*$^{+/+}$ littermates (□); *n* = 3–5 per genotype. *C*: Pancreatic islet circled by dashed line and Ki67-positive cells pointed by black arrow. RIPcre^{+}*fak*$^{fl/fl}$ islets (■) show a decreased percentage of Ki67-positive cells per islet compared with RIPcre^{+}*fak*$^{+/+}$ littermates (□; original magnification ×40); *n* = ~3,000 β-cells per animal from six 4–8-week-old mice per genotype were counted. *D*: Caspase 3 (Casp3) activation, as assessed by caspase 3 cleavage. Western blot of protein lysates of islets isolated from 4–8-week-old mice showing increased expression of activated caspase 3 in RIPcre^{+}*fak*$^{fl/fl}$ (■) compared with RIPcre^{+}*fak*$^{+/+}$ islets (□); *n* = 3 per genotype. *E*: RIPcre^{+}*fak*$^{fl/fl}$ mice (◆) were more susceptible to hyperglycemia than RIPcre^{+}*fak*$^{+/+}$ littermates (◇) after 2 days, but diminished at 14 days postinjection of multiple low doses of STZ, as shown by random blood glucose levels; *n* = 3–4 per genotype. *F*: Increased β-cell apoptosis in RIPcre^{+}*fak*$^{fl/fl}$ mice (■) compared with RIPcre^{+}*fak*$^{+/+}$ littermates (□) in basal state or after 2 days of injection of multiple low doses of STZ as assessed by TUNEL (original magnification ×40); *n* = ~1,000 β-cells per animal were counted from three to five 6–8-week-old male mice per genotype. **P* < 0.05; ***P* < 0.01; ****P* < 0.001. Results represent mean ± SE. +,+/+, RIPcre^{+}*fak*$^{+/+}$; +,−/−, RIPcre^{+}*fak*$^{fl/fl}$. wks, weeks. Scale bars, 40 μm. (A high-quality digital representation of this figure is available in the online issue.)

RIPcre^{+}*fak*$^{+/+}$ controls (Fig. 2*D* and *F*), indicating increased β-cell apoptosis under basal conditions. This, combined with reduced β-cell proliferation in islets of RIPcre^{+}*fak*$^{fl/fl}$ mice, is likely responsible for the decreased β-cell mass. In order to assess whether deletion of FAK in β-cells would also render these cells more susceptible to apoptotic stimuli, we challenged these mice with multiple low doses of STZ. Indeed, RIPcre^{+}*fak*$^{fl/fl}$ mice were more susceptible to hyperglycemia than RIPcre^{+}*fak*$^{+/+}$ littermates (Fig. 2*E*). An increase in random blood glucose levels of RIPcre^{+}*fak*$^{fl/fl}$ mice persisted post–STZ injections and remained significantly higher than RIPcre^{+}*fak*$^{+/+}$ controls throughout the 14-day period post–STZ injections. This was likely due to an increase in susceptibility to β-cell apoptosis, as evidenced by increased TUNEL-positive β-cells in the pancreas of RIPcre^{+}*fak*$^{fl/fl}$ mice compared with RIPcre^{+}*fak*$^{+/+}$ littermate controls (Fig. 2*F*).

FAK-deficient pancreatic β-cells show intact islet architecture but reduced insulin signaling. Given the role of FAK in integrin signaling and cell adhesion, linking communication between the ECM and the intracellular actin cytoskeleton, we next examined islet architecture in RIPcre^{+}*fak*$^{fl/fl}$ mice. Murine islets are characterized by a spherical structure containing insulin-producing β-cells in the core and other endocrine cells (α, ε, δ, and pancreatic polypeptide cells) in the periphery (20). By H&E staining and insulin-glucagon fluorescent coimmunostaining, islet architecture appeared intact in RIPcre^{+}*fak*$^{fl/fl}$ mice (Fig. 3*A*), and α-cell area and mass were similar between RIPcre^{+}*fak*$^{fl/fl}$ and RIPcre^{+}*fak*$^{+/+}$ mice (Fig. 3*B*). Given the role of FAK in integrin and insulin/PI3K signaling, we next assessed expression of signaling mediators in these pathways in isolated islets under basal conditions. Insulin and integrin signaling are regarded as critical molecular pathways in

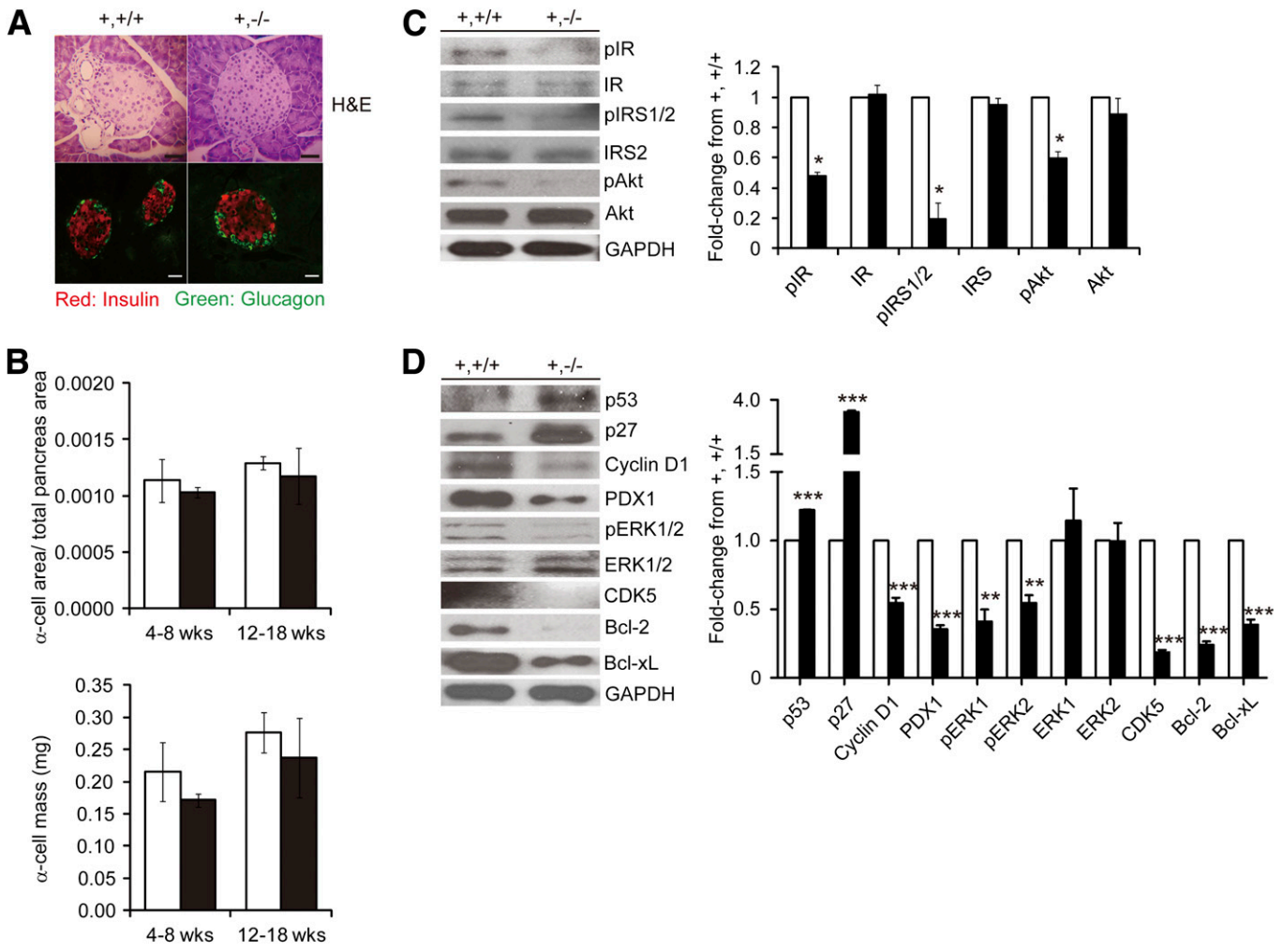

FIG. 3. Islet architecture and signal transduction pathways. *A*: Maintained islet architecture in RIPcre^{+}*fak*$^{fl/fl}$ islets as assessed by H&E staining and insulin/glucagon immunofluorescent costaining on pancreatic sections from 4–8-week-old mice (original magnification ×20); *n* = 3 per group. Scale bars, 40 μm. *B*: α-Cell area was quantified by glucagon-immunostained pancreatic sections and α-cell mass showed a similar level between RIPcre^{+}*fak*$^{fl/fl}$ mice (■) and RIPcre^{+}*fak*$^{+/+}$ littermates (□); *n* = 3 per genotype. *C*: Protein analysis by Western blot showed that RIPcre^{+}*fak*$^{fl/fl}$ islets have attenuated phosphorylated IR, IRS1/2, and Akt compared with RIPcre^{+}*fak*$^{+/+}$ littermates. GAPDH, glyceraldehyde-3-phosphate dehydrogenase. *D*: Protein analysis by Western blot showed that RIPcre^{+}*fak*$^{fl/fl}$ islets have attenuated ERK1/2 (ERK1 was referred to p44, as presented in the upper band of the Western blot image, and ERK2 was referred to p42, as presented in the bottom band of the image), cyclin D1, CDK5, Bcl-2, Bcl-xL, as well as PDX1, but increased expression of cell cycle inhibitors p53 and p27, compared with RIPcre^{+}*fak*$^{+/+}$ littermates. Islets were isolated from 4–8-week-old mice and used for Western blot analysis. Quantification analyses in right panel (□, RIPcre^{+}*fak*$^{+/+}$; ■, RIPcre^{+}*fak*$^{fl/fl}$); *n* = 3 per genotype. **P* < 0.05; ***P* < 0.01; ****P* < 0.001. Results represent mean ± SE. +,+/+, RIPcre^{+}*fak*$^{+/+}$; +,−/−, RIPcre^{+}*fak*$^{fl/fl}$. wks, weeks. (A high-quality digital representation of this figure is available in the online issue.)

regulating pancreatic β-cell proliferation, viability, and function (21,22). We observed that insulin signaling was suppressed in the islets of RIPcre^{+}*fak*$^{fl/fl}$ mice, as evidenced by a significant reduction in the phosphorylation levels of IR, IRS1/2, and Akt (Fig. 3*C*). Some target proteins of this signaling pathway relevant for cell cycle and apoptosis in β-cells (23–25), cyclin D1, p53, p27, and PDX-1, were also affected (Fig. 3*D*). In addition, reduced phosphorylation of ERK1/2, the main effector of integrin signaling, was also found in islets of RIPcre^{+}*fak*$^{fl/fl}$ mice. Interestingly, studies have shown that ERK is required for cell growth through regulating CDK5 expression and activation (26). Furthermore, CDK5/ERK signaling has been shown to activate Bcl-2/Bcl-xL expression to prevent apoptosis in neuronal cells (27). Here we found reduced CDK5, Bcl-2, and Bcl-xL expression levels in RIPcre^{+}*fak*$^{fl/fl}$ islets (Fig. 3*D*), suggesting that FAK plays a critical role in β-cell survival through regulating multiple signaling pathways that are involved in cell proliferation and apoptosis.

Impaired glucose-stimulated insulin secretion with normal GLUT2 and Ca^{2+} response in FAK-deficient β-cells. Insufficiency in either β-cell mass and/or function can lead to impaired glucose tolerance. Thus, we next examined whether FAK is also essential for β-cell function. Random plasma insulin level was decreased in RIPcre^{+}*fak*$^{fl/fl}$ mice (Fig. 4*A*) but similar insulin content was maintained within similarly sized islets (Fig. 4*B*). To further investigate β-cell function, we measured glucose-stimulated insulin secretion and found reduced insulin secretion in response to glucose in vitro (Fig. 4*C*). Phase I and phase II insulin secretion were also suppressed in vivo in RIPcre^{+}*fak*$^{fl/fl}$ mice (Fig. 4*D*). In response to glucose, multiple critical steps take place in β-cells, starting with glucose transport through GLUT2, followed by glucose metabolism and generation of ATP, resulting in closing of ATP-sensitive potassium (K_{ATP}) channels. Subsequent cell membrane depolarization activates voltage-dependent calcium channels, causing the influx of calcium ions

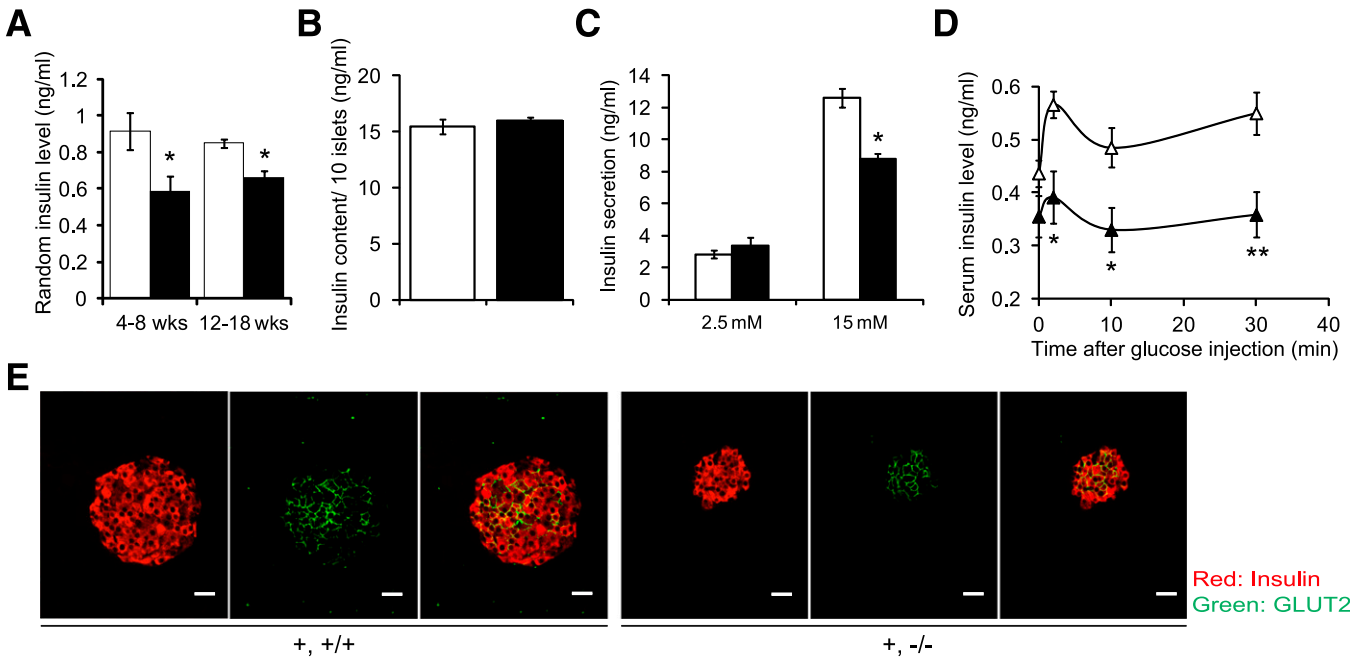

FIG. 4. Reduced insulin secretion in FAK-deficient β-cells with normal GLUT2 expression. *A*: Reduced random insulin level in RIPcre$^+$*fak*$^{fl/fl}$ (■) compared with RIPcre$^+$*fak*$^{+/+}$ littermates (□); *n* = 6 per genotype. Insulin content (*B*) and insulin secretion (*C*) in response to glucose (2.5 or 15 mmol/L), in group of 10 handpicked, similar-sized islets, were equal between RIPcre$^+$*fak*$^{+/+}$ (□) and RIPcre$^+$*fak*$^{fl/fl}$ (■) islets; *n* = 4 per genotype. *D*: Reduced insulin secretion in vivo after glucose stimulation in RIPcre$^+$*fak*$^{fl/fl}$ (▲) compared with RIPcre$^+$*fak*$^{+/+}$ littermates (△); *n* = 5–6 per genotype. *E*: Normal expression and distribution of GLUT2 on RIPcre$^+$*fak*$^{fl/fl}$ islets, as assessed by insulin/GLUT2 immunofluorescent costaining (original magnification ×20); *n* = 3 per genotype. Scale bars, 40 μm. **P* < 0.05; ***P* < 0.01. Results represent mean ± SE. All mice used in experiments were between 4 and 8 weeks of age. +,+/+, RIPcre$^+$*fak*$^{+/+}$; +,−/−, RIPcre$^+$*fak*$^{fl/fl}$. wks, weeks. (A high-quality digital representation of this figure is available in the online issue.)

that in turn stimulates insulin granule trafficking and exocytosis.

To investigate which aspects of glucose-stimulated insulin secretion were affected by absence of FAK, we first examined levels of GLUT2. Expression and distribution of GLUT2 in β-cells was similar between those of RIPcre$^+$*fak*$^{fl/fl}$ and RIPcre$^+$*fak*$^{+/+}$ mice (Fig. 4*E*). Furthermore, intracellular Ca^{2+} homeostasis, as evidenced by baseline Ca^{2+} levels and response to glucose (11 mmol/L), was similar between RIPcre$^+$*fak*$^{+/+}$ and RIPcre$^+$*fak*$^{fl/fl}$ islets (Fig. 5*A* and *B*). There was, however, an increase in the Ca^{2+} response to KCl in the RIPcre$^+$*fak*$^{fl/fl}$ islets, as shown in Fig. 5*A*. This was due to an increased density of voltage-dependent Ca^{2+} current in β-cells from RIPcre$^+$*fak*$^{fl/fl}$ islets (Fig. 5*C* and *D*). This increased activity in Ca^{2+} channels in response to KCl may reflect a compensatory mechanism to overcome insufficient insulin secretion. These results suggest that glucose sensing and Ca^{2+} response to glucose were normal in FAK-deficient β-cells.

Defective actin dynamics and decreased focal proteins in FAK-deficient β-cells. The normal Ca^{2+} response to glucose stimulation coupled with impaired insulin secretion in RIPcre$^+$*fak*$^{fl/fl}$ islets indicates that the functional defect in the islets might be due to impaired insulin granule trafficking. Since FAK is known to regulate the structure and function of F-actin (2), which is a key determinant controlling the access of insulin granules to the plasma membrane (28), we examined actin regulation in the β-cells of RIPcre$^+$*fak*$^{fl/fl}$ mice. At low glucose concentration (2.8 mmol/L), F-actin density was normally distributed in β-cells of RIPcre$^+$*fak*$^{+/+}$ and RIPcre$^+$*fak*$^{fl/fl}$ mice (Fig. 6*A*). Importantly, although glucose stimulation decreased cortical actin density in RIPcre$^+$*fak*$^{+/+}$ β-cells, there was no significant effect of glucose on cortical actin density in β-cells of RIPcre$^+$*fak*$^{fl/fl}$ mice. To further investigate this absent effect, we next examined paxillin and talin, which are focal proteins that regulate actin dynamics. These proteins can associate with FAK and form a linkage between integrin and F-actin filaments (29). We observed reduced expression levels of talin in RIPcre$^+$*fak*$^{fl/fl}$ islets (Fig. 6*B*). Paxillin can be directly activated by FAK and in our RIPcre$^+$*fak*$^{fl/fl}$ islets; we showed suppressed paxillin activity as evidenced by reduced phosphorylation at tyrosine 118 in both basal and glucose-stimulated conditions (Fig. 6*C*). In response to glucose, phospho-paxillin has been shown to colocalize with t-SNARE proteins, SNAP-25 and syntaxin 1, in primary β-cells (10). Consistent with the reduced phospho-paxillin expression by Western blot, RIPcre$^+$*fak*$^{fl/fl}$ β-cells showed reduced phospho-paxillin, which was colocalized with SNAP-25 or syntaxin 1 at the plasma membrane (Fig. 6*D*). These results demonstrate that the defect in glucose-stimulated insulin secretion is likely due to impaired glucose-dependent depolymerization of cortical actin through defective focal protein dynamics in β-cells of RIPcre$^+$*fak*$^{fl/fl}$ mice.

FAK-deficient β-cells have impaired insulin granule trafficking. The actin-formed dense web beneath the plasma membrane blocks insulin secretion by providing a barrier for the movement of insulin granules under low glucose concentrations (30,31). Upon glucose stimulation, actin undergoes depolymerization, allowing the granules to dock and fuse with the plasma membrane, resulting in insulin release. Our results in Fig. 6 show that cytoskeleton actin depolymerization was impaired in FAK-deficient β-cells, which suggests that insulin granule trafficking might be hampered due to defective actin dynamics. To assess insulin

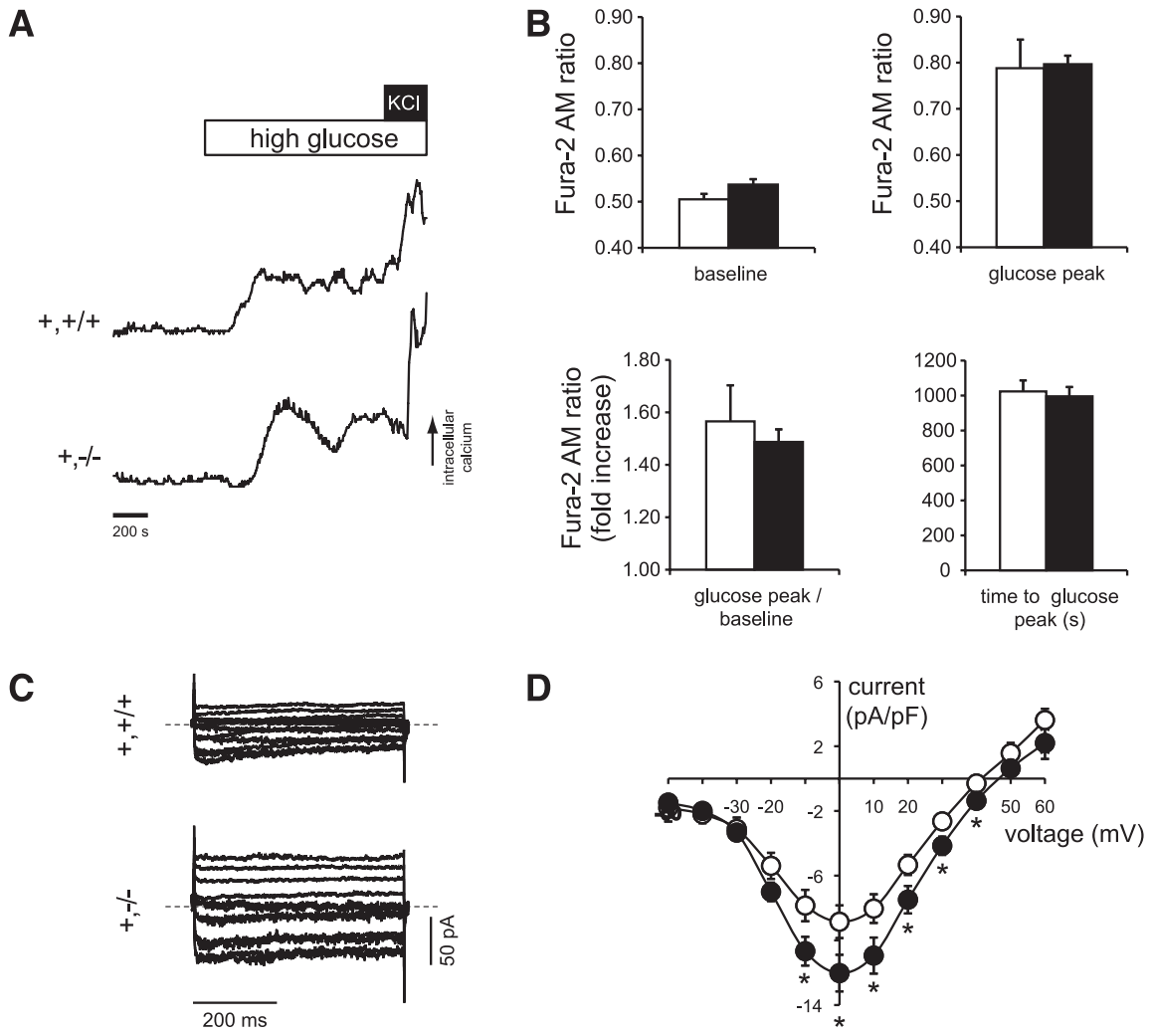

FIG. 5. Normal Ca^{2+} response in FAK-deficient β-cells. *A*: Intracellular Ca^{2+} responses, determined by ratiometric Fura-2-AM fluorescence measurements, were similar between RIPcre^{+}*fak*$^{+/+}$ and RIPcre^{+}*fak*$^{fl/fl}$ islets in response to glucose (11 mmol/L) and slightly increased in response to KCl (20 mmol/L). *B*: There were no differences in baseline or peak Fura-2-AM ratios, fold increase in response to 11 mmol/L glucose, or the time-to-peak response between RIPcre^{+}*fak*$^{+/+}$ (□) and RIPcre^{+}*fak*$^{fl/fl}$ (■) islets; *n* = 3 mice per genotype. *C*: Representative traces of voltage-gated Ca^{2+} currents measured in response to a series of increasing 500-ms depolarizations from −70 mV in single RIPcre^{+}*fak*$^{+/+}$ and RIPcre^{+}*fak*$^{fl/fl}$ β-cells. *D*: The current-voltage relationship, normalized to cell size, demonstrates a significant increase in Ca^{2+} current density (○, RIPcre^{+}*fak*$^{+/+}$; ●, RIPcre^{+}*fak*$^{fl/fl}$), which likely accounts for the increased intracellular Ca^{2+} response to KCl seen in *B*; *n* = 15–17 β-cells from three mice for each genotype. **P* < 0.05. Results represent mean ± SE. All mice used in experiments were between 4 and 8 weeks of age. +,+/+, RIPcre^{+}*fak*$^{+/+}$; +,−/−, RIPcre *fak*$^{fl/fl}$.

granule trafficking, we examined insulin granule localization in the RIPcre^{+}*fak*$^{fl/fl}$ β-cells by electron microscopy. A previous study indicates that insulin granules that reside within 0.2 μm of the plasma membrane can be morphologically considered docked granules (32). We found that under basal conditions, there were fewer insulin granules near the plasma membrane (<0.2 μm) in the β-cells of RIPcre^{+}*fak*$^{fl/fl}$ mice compared with RIPcre^{+}*fak*$^{+/+}$ mice (Fig. 7*A* and *B*). Upon glucose stimulation, the number of membrane-associated granules in RIPcre^{+}*fak*$^{+/+}$ β-cells increased significantly as expected, whereas in FAK-deficient β-cells, this failed to occur. Consistent with the notion that knockout of FAK results in fewer docked insulin granules at the plasma membrane of β-cells, we observed a reduced exocytotic response in single β-cells from RIPcre^{+}*fak*$^{fl/fl}$ islets in response to a series of 10 membrane depolarizations from −70 to 0 mV (Fig. 8*A* and *B*), demonstrating that FAK may regulate actin dynamics in vivo to control insulin granule trafficking and insulin secretion in pancreatic β-cells.

DISCUSSION

Null mutation of FAK causes embryonic lethality in the early developmental period, supporting the critical role of FAK in multiple cellular processes (33). To gain insight into the in vivo role of FAK in pancreatic β-cell homeostasis, we developed mice with β-cell–specific deletion of FAK using the Cre-loxP recombination system. In this study, we show that these mice have reduced β-cell mass and exhibit a defect in glucose-stimulated insulin secretion, which together result in impaired glucose tolerance. The reduction in β-cell mass results from a concomitant downregulation of proliferation and upregulation of apoptosis, whereas insufficient insulin secretion appears to be due to the impaired control of actin dynamics and reduced insulin granule trafficking to the plasma membrane.

FAK coordinates signals from growth factor receptors, such as those for insulin or epidermal growth factor, to regulate cell growth and survival. As such, disruption of FAK activates p53, the cell cycle progression inhibitor, in

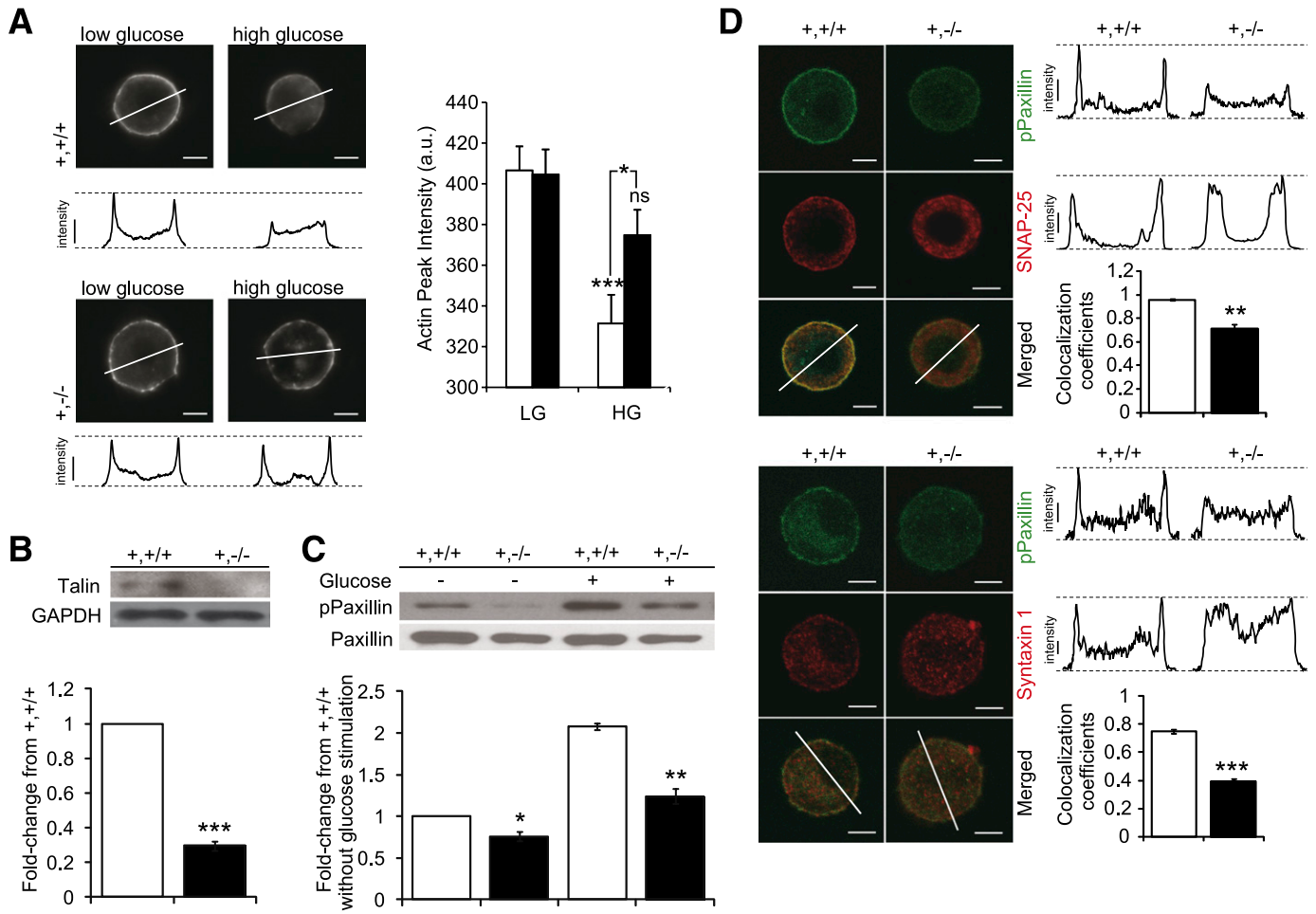

FIG. 6. Deletion of FAK in β-cells results in impaired actin depolymerization and reduced phosphorylated paxillin (pPaxillin) and talin expression levels. ***A*: F-actin, detected by staining with Alexa Fluor 488–conjugated phalloidin, was depolymerized by high glucose (16.7 mmol/L) in β-cells from RIPcre^{+}*fak*$^{+/+}$ (□) but not RIPcre^{+}*fak*$^{fl/fl}$ (■) mice. Cells were confirmed as β-cells by positive immunostaining for insulin (not shown). The peak intensity of F-actin staining at the plasma membrane was quantified and expressed as arbitrary units (a.u.); *n* = 72–115 β-cells from three mice for each genotype. HG, high glucose; LG, low glucose. *B*: Reduced talin expression in RIPcre^{+}*fak*$^{fl/fl}$ (■) islets compared with RIPcre^{+}*fak*$^{+/+}$ (□) littermates; *n* = 3 per genotype. *C*: Suppressed phosphorylation of paxillin expression with or without glucose stimulation (15 mmol/L) in RIPcre^{+}*fak*$^{fl/fl}$ (■) islets compared with RIPcre^{+}*fak*$^{+/+}$ (□) littermates as assessed by Western blot. Quantification analyses in bottom panel; *n* = 3 per genotype. *D*: β-Cells were stimulated by glucose (15 mmol/L) for 20 min and stained for phospho-paxillin (green) and syntaxin 1 or SNAP-25 (red); *n* = 3 per genotype (□, RIPcre^{+}*fak*$^{+/+}$; ■, RIPcre^{+}*fak*$^{fl/fl}$). Scale bars, 5 μm. All mice used in experiments were between 4 and 8 weeks of age. *$P < 0.05$; **$P < 0.01$; ***$P < 0.001$. Results represent mean ± SE. +,+/+, RIPcre^{+}*fak*$^{+/+}$; +,−/−, RIPcre^{+}*fak*$^{fl/fl}$. (A high-quality digital representation of this figure is available in the online issue.)**

endothelial cells during mouse embryogenesis (34). Cell cycle–regulating proteins p27 and cyclin D1 were shown to be required for FAK-dependent cell cycle progression in glioblastoma cells (24). FAK has also been identified as a critical mediator of insulin signaling (7–9), participating in IR phosphorylation (35) and activating PI3K/Akt (36,37) through phosphorylating the p85 subunit of PI3K, suggesting that FAK might associate with IRS/PI3K to activate insulin signaling and deletion of FAK in β-cells may directly attenuate insulin/Akt signaling, as shown in this study.

Genome-wide association studies have identified CDK5 regulatory subunit–associated protein-like 1 (CDKAL1) as one of the genes associated with the development of type 2 diabetes (38). A recent report indicates that siRNA knockdown of CDK5 expression in a rat insulinoma cell line (INS 832/13) leads to enhanced apoptosis through decreased activation of FAK, resulting in attenuation of the PI3K/Akt survival pathway (39). ERK is required for CDK5 expression (26) and the CDK5/ERK pathway is responsible for upregulation of antiapoptotic protein Bcl-2 and Bcl-xL (27). Consistent with these observations, FAK deletion in β-cells leads to increased susceptibility of apoptosis, suggesting FAK/ERK/CDK5 signaling to be crucial for β-cell survival. Furthermore, decreased phosphorylated FAK^{Ser732} expression was observed in pancreas sections of humans with type 2 diabetes (39), which confirms that the activity of FAK is important for β-cell survival and may play a causal role in the development of type 2 diabetes. The results presented here support the notion that reduced FAK activity in β-cells can play a role in diabetes pathogenesis.

During the process of glucose-stimulated insulin secretion, pancreatic β-cells have been observed to undergo focal adhesion remodeling similar to the events that occur during cell migration (10). Upon glucose stimulation, paxillin is phosphorylated by activated FAK, and both of these activated focal proteins migrate to the plasma membrane at the newly formed filopodia in primary β-cells (10). Interestingly, phospho-paxillin has been shown to connect with F-actin at focal adhesions (40). Together, actin dynamics

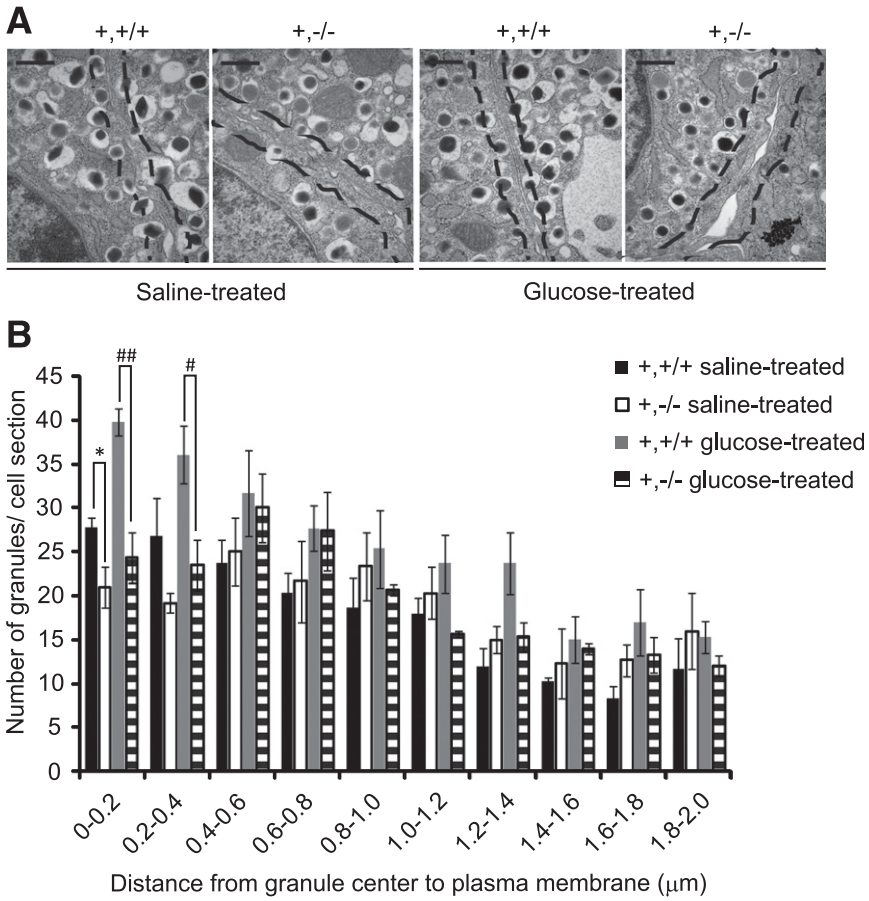

FIG. 7. Impaired insulin granule trafficking in FAK-deficient β-cells leads to a lower number of docked insulin granules. *A*: Electron micrographs of β-cell sections. Scale bar, 500 nm. Black dashed lines indicate a distance of 200 nm from the plasma membrane, showing that β-cells of RIPcre^{+}*fak*$^{fl/fl}$ mice have a fewer number of insulin granules docked at the plasma membrane in both saline-treated or glucose-treated (15 mmol/L) conditions. *B*: Quantification of relative granule distribution and density in the first 2-μm region adjacent to the plasma membrane; *n* = ~2,000 insulin granules from 12–15 β-cells were counted from three mice per genotype. *Comparison between saline-treated RIPcre^{+}*fak*$^{+/+}$ and RIPcre^{+}*fak*$^{fl/fl}$ islets. #Comparison between glucose-treated RIPcre^{+}*fak*$^{+/+}$ and RIPcre^{+}*fak*$^{fl/fl}$ islets. *,#*P* < 0.05; ##*P* < 0.01. Results represent mean ± SE. All mice used in experiments were between 4 and 8 weeks of age. +,+/+, RIPcre^{+}*fak*$^{+/+}$; +,−/−, RIPcre^{+}*fak*$^{fl/fl}$.

is a complex process that is critical for glucose-stimulated insulin secretion (4,31). Here, we show that FAK can regulate focal protein dynamics, which in turn can control cortical F-actin depolymerization in response to glucose. Additionally, phosphorylation of paxillin has also been considered to be important in globular actin/F-actin transition (41). In this study, we found reduced phospho-paxillin levels in basal and glucose-stimulated conditions in RIPcre^{+}*fak*$^{fl/fl}$ islets and decreased colocalization of phospho-paxillin with plasma membrane t-SNARE proteins SNAP-25 and syntaxin 1 in RIPcre^{+}*fak*$^{fl/fl}$ β-cells. These SNARE proteins are thought to be involved in regulating insulin granule fusion to

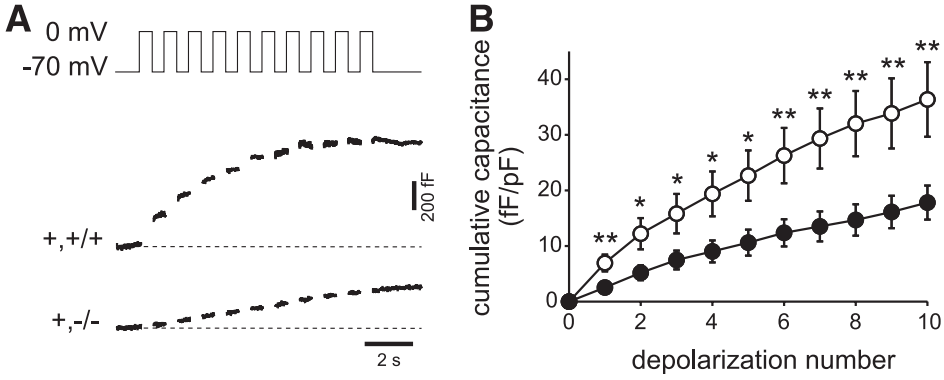

FIG. 8. Impaired exocytotic responses in FAK-deficient β-cells. *A*: Representative capacitance responses elicited from single β-cells from RIPcre^{+}*fak*$^{+/+}$ and RIPcre^{+}*fak*$^{fl/fl}$ mice in response to a series of ten 500-ms depolarizations from −70 to 0 mV. *B*: Averaged data demonstrates an impaired exocytotic response in β-cells from the RIPcre^{+}*fak*$^{fl/fl}$ mice (●) compared with those from RIPcre^{+}*fak*$^{+/+}$ mice (○); *n* = 18–24 β-cells from three mice of each genotype. All mice used in experiments were between 4 and 8 weeks of age. **P* < 0.05; ***P* < 0.01. Results represent mean ± SE. +,+/+, RIPcre^{+}*fak*$^{+/+}$; +,−/−, RIPcre^{+}*fak*$^{fl/fl}$.

the plasma membrane (42) and are linked to the actin cytoskeleton (43). Thus, in response to glucose, FAK phosphorylates and activates paxillin, which localizes with t-SNAREs to regulate cortical F-actin depolymerization, in turn facilitating insulin granule trafficking and exocytosis.

Talin acts as the key component for integrin-actin linkage and focal adhesion assembly (44). Talin can directly bind to integrin cytoplasmic tails and FAK by its NH_2-terminal head domain and actin filament by either NH_2- or COOH-terminal rod domains (29). Downregulation of talin expression by siRNA in HeLa cells slows the kinetics of cell spreading and prolongs the process time of β1 integrin maturation (45), which can upregulate Bcl-2 expression (46), and has been identified as a critical factor for maintain β-cell survival and function (21). These studies suggest that talin may play an important role not only in cytoskeleton remodeling but also in cell proliferation. The talin expression level can be modulated by mechanical stimuli through nitric oxide synthase activity (47), which has been shown to be induced by the integrin/FAK/Src/ERK pathway to regulate cell migration (48,49). Accordingly, we observed reduced talin expression in the RIPcre^{+}*fak*$^{fl/fl}$ islets, suggesting that FAK is essential in regulating talin expression, which in turn can contribute to impaired β-cell function by affecting actin dynamics and reducing β-cell viability.

Altogether, in this study, we show for the first time that FAK is required for the maintenance of both pancreatic β-cell mass and function in vivo, such that in its absence, glucose homeostasis is perturbed. We show that deletion of FAK in β-cells results in impaired cell proliferation, survival, and function. The reduced insulin exocytosis in the absence of FAK is likely due to defects in actin dynamics through impaired focal protein dynamics, resulting in insufficient insulin granule trafficking. We demonstrate in vivo that FAK has a critical dual role in regulating both β-cell viability and cell function, and may be a potential therapeutic target for type 2 diabetes.

ACKNOWLEDGMENTS

This work was supported by Canadian Institutes of Health Research (CIHR) operating grants MOP-201188 and MOP-191501 to M.W. and a Canadian Diabetes Association (CDA) grant-in-aid to P.E.M. E.P.C. is supported by the CDA Doctoral Student Research Award. M.C. is supported by a fellowship from Alberta Innovates-Health Solutions (AI-HS). C.T.L. is supported by the Eliot Phillipson Clinician Scientist Training program and the Banting and Best Diabetes Centre (BBDC) postdoctoral fellowship. S.Y.S. is supported by the BBDC–Novo Nordisk Studentship and the Natural Sciences and Engineering Research Council Alexander Graham Bell Canada Graduate Scholarship. C.H. is supported by a studentship from CIHR and AI-HS. P.E.M. is an AI-HS Scholar and holds the Canada Research Chair in Islet Biology.

No potential conflicts of interest relevant to this article were reported.

E.P.C. generated and analyzed research data and prepared the manuscript. M.C., S.A.S., D.C., X.Q.D., C.H., A.F.S., and D.Z. generated research data. C.T.L. and S.Y.S. generated research data and edited the manuscript. H.Y.G., P.E.M., and M.W. designed experiments, supervised students, contributed to discussion and interpretation of the data, and reviewed and edited the manuscript. M.W. is the guarantor of this work and, as such, had full access to all the data in the study and takes responsibility for the integrity of the data and the accuracy of the data analysis.

This study was presented as a guided audio poster at the 71st Scientific Sessions of the American Diabetes Association, San Diego, California, 24–28 June 2011.

The authors thank Dr. Shun Yan Lu (Ontario Cancer Institute, Toronto, Ontario, Canada) and Nancy Smith (University of Alberta) for their technical assistance.

REFERENCES

1. Schaller MD, Borgman CA, Cobb BS, Vines RR, Reynolds AB, Parsons JT. pp125FAK a structurally distinctive protein-tyrosine kinase associated with focal adhesions. Proc Natl Acad Sci USA 1992;89:5192–5196
2. Mitra SK, Hanson DA, Schlaepfer DD. Focal adhesion kinase: in command and control of cell motility. Nat Rev Mol Cell Biol 2005;6:56–68
3. Thurmond DC, Gonelle-Gispert C, Furukawa M, Halban PA, Pessin JE. Glucose-stimulated insulin secretion is coupled to the interaction of actin with the t-SNARE (target membrane soluble N-ethylmaleimide-sensitive factor attachment protein receptor protein) complex. Mol Endocrinol 2003;17:732–742
4. Li G, Rungger-Brändle E, Just I, Jonas JC, Aktories K, Wollheim CB. Effect of disruption of actin filaments by *Clostridium botulinum* C2 toxin on insulin secretion in HIT-T15 cells and pancreatic islets. Mol Biol Cell 1994; 5:1199–1213
5. Lim ST, Mikolon D, Stupack DG, Schlaepfer DD. FERM control of FAK function: implications for cancer therapy. Cell Cycle 2008;7:2306–2314
6. McLean GW, Carragher NO, Avizienyte E, Evans J, Brunton VG, Frame MC. The role of focal-adhesion kinase in cancer—a new therapeutic opportunity. Nat Rev Cancer 2005;5:505–515
7. Bisht B, Srinivasan K, Dey CS. In vivo inhibition of focal adhesion kinase causes insulin resistance. J Physiol 2008;586:3825–3837
8. Bisht B, Dey CS. Focal adhesion kinase contributes to insulin-induced actin reorganization into a mesh harboring glucose transporter-4 in insulin resistant skeletal muscle cells. BMC Cell Biol 2008;9:48
9. Bisht B, Goel HL, Dey CS. Focal adhesion kinase regulates insulin resistance in skeletal muscle. Diabetologia 2007;50:1058–1069
10. Rondas D, Tomas A, Halban PA. Focal adhesion remodeling is crucial for glucose-stimulated insulin secretion and involves activation of focal adhesion kinase and paxillin. Diabetes 2011;60:1146–1157
11. Postic C, Shiota M, Niswender KD, et al. Dual roles for glucokinase in glucose homeostasis as determined by liver and pancreatic beta cell-specific gene knock-outs using Cre recombinase. J Biol Chem 1999;274: 305–315
12. Le May C, Chu K, Hu M, et al. Estrogens protect pancreatic beta-cells from apoptosis and prevent insulin-deficient diabetes mellitus in mice. Proc Natl Acad Sci USA 2006;103:9232–9237
13. Choi D, Schroer SA, Lu SY, Cai EP, Hao Z, Woo M. Redundant role of the cytochrome c-mediated intrinsic apoptotic pathway in pancreatic β-cells. J Endocrinol 2011;210:285–292
14. Choi D, Schroer SA, Lu SY, et al. Erythropoietin protects against diabetes through direct effects on pancreatic beta cells. J Exp Med 2010;207:2831–2842
15. Wang L, Liu Y, Yan Lu S, et al. Deletion of Pten in pancreatic ß-cells protects against deficient ß-cell mass and function in mouse models of type 2 diabetes. Diabetes 2010;59:3117–3126
16. Choi D, Cai EP, Schroer SA, Wang L, Woo M. Vhl is required for normal pancreatic β cell function and the maintenance of β cell mass with age in mice. Lab Invest 2011;91:527–538
17. Dai XQ, Plummer G, Casimir M, et al. SUMOylation regulates insulin exocytosis downstream of secretory granule docking in rodents and humans. Diabetes 2011;60:838–847
18. Kwan EP, Gaisano HY. Glucagon-like peptide 1 regulates sequential and compound exocytosis in pancreatic islet beta-cells. Diabetes 2005;54:2734–2743
19. Wicksteed B, Brissova M, Yan W, et al. Conditional gene targeting in mouse pancreatic β-cells: analysis of ectopic Cre transgene expression in the brain. Diabetes 2010;59:3090–3098
20. Baetens D, Malaisse-Lagae F, Perrelet A, Orci L. Endocrine pancreas: three-dimensional reconstruction shows two types of islets of Langerhans. Science 1979;206:1323–1325
21. Riopel M, Krishnamurthy M, Li J, Liu S, Leask A, Wang R. Conditional β1-integrin-deficient mice display impaired pancreatic β cell function. J Pathol 2011;224:45–55
22. Kulkarni RN, Brüning JC, Winnay JN, Postic C, Magnuson MA, Kahn CR. Tissue-specific knockout of the insulin receptor in pancreatic beta cells creates an insulin secretory defect similar to that in type 2 diabetes. Cell 1999;96:329–339

23. Lim ST, Chen XL, Lim Y, et al. Nuclear FAK promotes cell proliferation and survival through FERM-enhanced p53 degradation. Mol Cell 2008;29:9–22
24. Ding Q, Grammer JR, Nelson MA, Guan JL, Stewart JE Jr, Gladson CL. p27Kip1 and cyclin D1 are necessary for focal adhesion kinase regulation of cell cycle progression in glioblastoma cells propagated in vitro and in vivo in the scid mouse brain. J Biol Chem 2005;280:6802–6815
25. Hui H, Perfetti R. Pancreas duodenum homeobox-1 regulates pancreas development during embryogenesis and islet cell function in adulthood. Eur J Endocrinol 2002;146:129–141
26. Harada T, Morooka T, Ogawa S, Nishida E. ERK induces p35, a neuron-specific activator of Cdk5, through induction of Egr1. Nat Cell Biol 2001;3:453–459
27. Wang CX, Song JH, Song DK, Yong VW, Shuaib A, Hao C. Cyclin-dependent kinase-5 prevents neuronal apoptosis through ERK-mediated upregulation of Bcl-2. Cell Death Differ 2006;13:1203–1212
28. Pigeau GM, Kolic J, Ball BJ, et al. Insulin granule recruitment and exocytosis is dependent on p110gamma in insulinoma and human beta-cells. Diabetes 2009;58:2084–2092
29. Le Clainche C, Carlier MF. Regulation of actin assembly associated with protrusion and adhesion in cell migration. Physiol Rev 2008;88:489–513
30. Orci L, Gabbay KH, Malaisse WJ. Pancreatic beta-cell web: its possible role in insulin secretion. Science 1972;175:1128–1130
31. Nevins AK, Thurmond DC. Glucose regulates the cortical actin network through modulation of Cdc42 cycling to stimulate insulin secretion. Am J Physiol Cell Physiol 2003;285:C698–C710
32. Gomi H, Mizutani S, Kasai K, Itohara S, Izumi T. Granuphilin molecularly docks insulin granules to the fusion machinery. J Cell Biol 2005;171:99–109
33. Ilić D, Furuta Y, Kanazawa S, et al. Reduced cell motility and enhanced focal adhesion contact formation in cells from FAK-deficient mice. Nature 1995;377:539–544
34. Ilic D, Kovacic B, McDonagh S, et al. Focal adhesion kinase is required for blood vessel morphogenesis. Circ Res 2003;92:300–307
35. El Annabi S, Gautier N, Baron V. Focal adhesion kinase and Src mediate integrin regulation of insulin receptor phosphorylation. FEBS Lett 2001;507:247–252
36. Xia H, Nho RS, Kahm J, Kleidon J, Henke CA. Focal adhesion kinase is upstream of phosphatidylinositol 3-kinase/Akt in regulating fibroblast survival in response to contraction of type I collagen matrices via a beta 1 integrin viability signaling pathway. J Biol Chem 2004;279:33024–33034
37. Lebrun P, Mothe-Satney I, Delahaye L, Van Obberghen E, Baron V. Insulin receptor substrate-1 as a signaling molecule for focal adhesion kinase pp125(FAK) and pp60(src). J Biol Chem 1998;273:32244–32253
38. Petrie JR, Pearson ER, Sutherland C. Implications of genome wide association studies for the understanding of type 2 diabetes pathophysiology. Biochem Pharmacol 2011;81:471–477
39. Daval M, Gurlo T, Costes S, Huang CJ, Butler PC. Cyclin-dependent kinase 5 promotes pancreatic β-cell survival via Fak-Akt signaling pathways. Diabetes 2011;60:1186–1197
40. Nakamura K, Yano H, Uchida H, Hashimoto S, Schaefer E, Sabe H. Tyrosine phosphorylation of paxillin alpha is involved in temporospatial regulation of paxillin-containing focal adhesion formation and F-actin organization in motile cells. J Biol Chem 2000;275:27155–27164
41. Tang DD, Turner CE, Gunst SJ. Expression of non-phosphorylatable paxillin mutants in canine tracheal smooth muscle inhibits tension development. J Physiol 2003;553:21–35
42. Jewell JL, Oh E, Thurmond DC. Exocytosis mechanisms underlying insulin release and glucose uptake: conserved roles for Munc18c and syntaxin 4. Am J Physiol Regul Integr Comp Physiol 2010;298:R517–R531
43. Jewell JL, Luo W, Oh E, Wang Z, Thurmond DC. Filamentous actin regulates insulin exocytosis through direct interaction with syntaxin 4. J Biol Chem 2008;283:10716–10726
44. Giannone G, Jiang G, Sutton DH, Critchley DR, Sheetz MP. Talin1 is critical for force-dependent reinforcement of initial integrin-cytoskeleton bonds but not tyrosine kinase activation. J Cell Biol 2003;163:409–419
45. Albigès-Rizo C, Frachet P, Block MR. Down regulation of talin alters cell adhesion and the processing of the alpha 5 beta 1 integrin. J Cell Sci 1995;108:3317–3329
46. Zhang Z, Vuori K, Reed JC, Ruoslahti E. The alpha 5 beta 1 integrin supports survival of cells on fibronectin and up-regulates Bcl-2 expression. Proc Natl Acad Sci USA 1995;92:6161–6165
47. Tidball JG, Spencer MJ, Wehling M, Lavergne E. Nitric-oxide synthase is a mechanical signal transducer that modulates talin and vinculin expression. J Biol Chem 1999;274:33155–33160
48. Gupta SK, Vlahakis NE. Integrin alpha9beta1 mediates enhanced cell migration through nitric oxide synthase activity regulated by Src tyrosine kinase. J Cell Sci 2009;122:2043–2054
49. Ajizian SJ, English BK, Meals EA. Specific inhibitors of p38 and extracellular signal-regulated kinase mitogen-activated protein kinase pathways block inducible nitric oxide synthase and tumor necrosis factor accumulation in murine macrophages stimulated with lipopolysaccharide and interferon-gamma. J Infect Dis 1999;179:939–944